Impression

lundi 26 octobre 2020 14:07

Influence of the heated blocks on the natural convection in 3D cylindrical and divergent annular duct

Souad Benkherbache*

Department of Mechanical Engineering,
University of M'sila,
28000, Algeria
Email: soucief@yahoo.fr
*Corresponding author

Mohamed Si-Ameur

LESEI,
Department of Mechanical Engineering,
University of Batna,
05000, Algeria
Email: msiameur@yahoo.fr

Abstract: In this paper, a numerical investigation of natural convection in three-dimensional cylindrical and divergent annular duct is studied. In the inner cylinder of thin thickness, are mounted a cylindrical blocks which subjected to a volumetric heat generation. The governing equations of mass, momentum and energy equation for both the fluid and the solid are solved by the finite volume method using the commercially available CFD software fluent .The effect of the number of heated blocks (N = 1, 2, 3 and 5) and the inclination angle of the divergent (ϕ = 0°, 15°, 23° and 45°) have been studied . The temperature and velocity contours fields, stream lines also the local Nusselt number have been presented here for Ra = 2.10^5 and N = 3 while temperature and velocity profiles in the span-wise direction of the flow were plotted for Ra = 1.10^5 (ϕ = 0°, 15°, 23° and 45°) and (N = 1, 2, 3 and 5) also the local and average Nusselt number for those geometries.

Keywords: natural convection; annular space; divergent duct; volumetric heat generation; heat sink; CFD.

Reference to this paper should be made as follows: Benkherbache, S. and Si-Ameur, M. (2017) 'Influence of the heated blocks on the natural convection in 3D cylindrical and divergent annular duct', *Int. J. Engineering Systems Modelling and Simulation*, Vol. 9, No. 1, pp.20–31.

Biographical notes: Souad Benkherbache is a Lecturer Assistant in M'sila University where she received her MSc in 2005. Currently, she is a PhD student in M'sila University. Her area of interests is computational fluid dynamic and heat transfer.

Mohamed Si-Ameur received his PhD from Joseph Fourier University of Grenoble (France) in 1994 and worked as part-time researcher and teacher in Grenoble academy. Currently, he is a Professor of Mechanics in Batna University. His major researches interests are in incompressible and compressible turbulent flows.

1 Introduction

The concentric annular duct is an important geometry of many fluid flows and heat transfer devices. The study of natural convection in this configuration is important from both theoretical and practical point of view. The fluid dynamic behaviour of air in open environments with or without the presence or not heat generating sources is extensively applicable, in industrial environments, nuclear reactors, solar energy collectors, energy storage, electronic equipment's, and energy storage. Cooling by natural convection over heated bodies or fins in horizontal and vertical channel, have received considerable attention and have been experimentally and numerically studied by many researchers (e.g., Edwards et al., 1963; Rasim, 1996; Chen, 2007; Bazylak, 2007).

Adding a fin to an object increases the amount of surface area in contact with the surrounding fluid, which increases the heat transfer between the object and the surrounding fluid. Heated bodies can be used in variety applications such as heat sinks and heat exchangers. The performance of any heat sink is measured by the

temperature difference between its base and the ambient temperature normalised to the dissipated power. This performance is a strong function of the operating environment, material, geometry, and overall surface heat transfer coefficient. Heat sinks are used in a wide range of applications wherever efficient heat dissipation is required, major examples include refrigeration, heat engines, cooling electronic devices and lasers. Microprocessors and power handling semiconductors are examples of electronics that need a heat sink to reduce their temperature through increased thermal mass and heat dissipation (primarily by conduction and convection and to a lesser extent by radiation). Cooling electronic components using natural convection is considerably more challenging than forced air cooling, that is because the thermal resistance of a heat sink may be up to 20% higher in a natural convection environment than in a forced convection environment. In natural convection, the heat sink depends solely on the 'chimney effect' to break the layers of still air and accelerate the cold air circulation over the heat sink. The existing literature presents a vast number of studies on convection in its three forms and in open or closed cavities. Dehghan et al. (1996) investigated the influence of the heating generation mode and the separation distances between the sources in their numerical modelling of natural convection air cooling. Kasayapanand (2009) investigated a numerical modelling of the electric field effect, on natural convection in finned enclosures; he analysed the interaction between electric fields flow and temperature. Kobus et al. (2005) developed experimental technique parameters for pure natural convection and for combined forced and natural convection. Amir et al. (2010) studied numerically the convection cooling of horizontal heat source mounted in square cavity filled with nano fluid, their results shows that dimension of heat source is an important parameter affecting the flow pattern and temperature fields. Wang et al. (1999) presented a procedure for the development of a comprehensive model for natural convection heat transfer from isothermal vertical disks with horizontal support cylinders as found in annular fin heat sinks. Culham et al. (2000) presented an analytical model for calculating natural convection heat transfer for three heat sinks geometries.

Catharina et al. (2001) provided a system and method for enhancing thermal performance of a heat transfer device. The most effective heat transfer enhancement can be achieved by using fins as elements for the heat transfer surface area extension. A large variety of fins have been applied for this purpose, the area of interest is a tube fin configuration. the aim of this work is to study the heat transfer enhancement of fin tube immersed in a cylindrical or divergent tube, here the fins are considered as a cylindrical generating blocks and the divergent configuration is provided for enhancing thermal performance of a heat transfer device. So this kind of configuration has not been yet studied, and the purpose of the present work is to study the buoyancy driven flow generated by heated blocks in a three dimensional cylindrical and divergent annular duct. In the inner thin cylinder are fixed cylindrical blocks subjected to a volumetric heat generation, while the opposite wall of the outer cylinder which is inclined is supposed adiabatic. This work aims to study the effect of the number of heated blocks and the inclination angle of the outer cylinder on the flow and heat transfer characteristics (Figure 1).

Figure 1 Studied configuration (see on line version for colours)

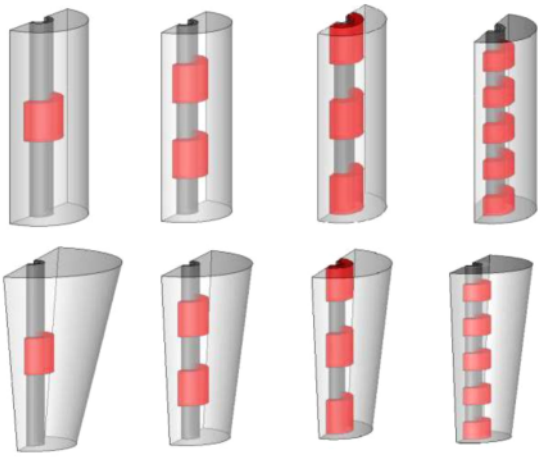

Figure 2 Schematic view of the physical problem (see online version for colours)

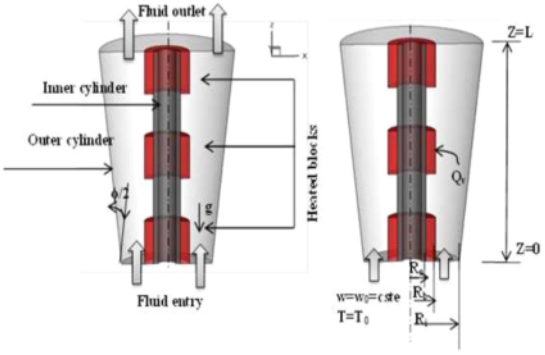

2 Problem configuration

The physical model illustrated in Figure 2 consists of a vertical annular and divergent duct. In the external wall of the inner cylinder are mounted a cylindrical blocks which are submitted to uniform volumetric heat generation. The three-dimensional configuration was defined by exploiting the symmetry of the duct; a vertical symmetry plane allows reducing the computational domain to the total half-volume. The fluid entering by the bottom with constant velocity w_0 and at ambient temperature T_0 while the annular space is open in top to the atmospheric pressure.

The geometric parameters are fixed throughout the parametric study. The dimensions considered in the present study are as follows: The length of the duct L = 50 mm, the radius of the inner cylinder R_i = 3 mm, the radius of the block R_b = 5 mm and the radius of the outer cylinder R_o = 10 mm. The fluid, air (the Prandtl number Pr = 0.71) is brought to initial temperature T_0 = 298 K.

2.1 Governing equations

The flow and temperature distributions are governed by continuity, Navier-Stokes, fluid and the fluid-solid energy equations. The flow is steady; the fluid is Newtonian and incompressible, with constant properties, except in the term of gravity where the Boussinesq assumption is adopted).The thermo physical properties of the fluid are constant and evaluated at inlet temperature. Radiation transfers and viscous dissipations are supposed negligible. Considering of the simplifying assumptions formulated above, the governing equations in cylindrical coordinates in directions (r, θ, and z) Bejan (1995) are as follows:

- continuity equation

$$\frac{1}{r}\frac{\partial u}{\partial r}+\frac{1}{r}\frac{\partial v}{\partial \theta}+\frac{\partial w}{\partial z}=0 \tag{1}$$

- momentum equation

$$\rho\left(\frac{\partial u}{\partial r}+\frac{v}{r}\frac{\partial u}{\partial \theta}+w\frac{\partial u}{\partial z}-\frac{v^2}{r}\right) = -\frac{\partial p}{\partial r}+\mu\left[\frac{\partial}{\partial r}\left(\frac{1}{r}\frac{\partial}{\partial r}(ru)\right)+\frac{1}{r^2}\frac{\partial^2 u}{\partial \theta^2}-\frac{2}{r^2}\frac{\partial v}{\partial \theta}+\frac{\partial^2 u}{\partial z^2}\right] \tag{2}$$

$$\rho\left(u\frac{\partial v}{\partial r}+\frac{v}{r}\frac{\partial v}{\partial \theta}+w\frac{\partial v}{\partial z}+\frac{uv}{r}\right) = -\frac{1}{r}\frac{\partial p}{\partial \theta}+\mu\left[\frac{\partial}{\partial r}\left(\frac{1}{r}\frac{\partial}{\partial r}(rv)\right)+\frac{1}{r^2}\frac{\partial^2 v}{\partial \theta^2}+\frac{2}{r^2}\frac{\partial u}{\partial \theta}+\frac{\partial^2 v}{\partial z^2}\right] \tag{3}$$

$$\rho\left(u\frac{\partial w}{\partial r}+\frac{v}{r}\frac{\partial v}{\partial \theta}+w\frac{\partial v}{\partial z}\right) = -\frac{\partial p}{\partial z}+\mu\left[\frac{1}{r}\frac{\partial}{\partial r}\left(r\frac{\partial w}{\partial r}\right)+\frac{1}{r^2}\frac{\partial^2 w}{\partial \theta^2}+\frac{\partial^2 w}{\partial z^2}\right] + \rho g\beta\left(T-T_0\right) \tag{4}$$

- energy equation

$$\frac{1}{r}\frac{\partial(ruT)}{\partial r}+\frac{1}{r}\frac{\partial(vT)}{\partial \theta}+\frac{\partial(wT)}{\partial z} = \frac{k_f}{(\rho C_p)}\left[\frac{1}{r}\frac{\partial}{\partial r}\left(r\frac{\partial T}{\partial r}\right)+\frac{1}{r^2}\frac{\partial^2 T}{\partial \theta^2}+\frac{\partial^2 T}{\partial z^2}\right] \tag{5}$$

- energy equation for the solid wall

$$k_s\left[\frac{1}{r}\frac{\partial}{\partial r}\left(\frac{\partial T}{\partial r}\right)+\frac{1}{r^2}\frac{\partial^2 T}{\partial \theta^2}+\frac{\partial^2 T}{\partial z^2}\right]=Q_v. \tag{6}$$

2.2 Boundary conditions

The velocity boundary condition is (u = v = w = 0) for the walls of the duct and the blocks.

For the fluid the temperature is $T = T_0$.

For the adiabatic walls of the inner and outer cylinder.

$$\frac{\partial T}{\partial n}=0$$

- At interface solid fluid

$$-k_f\frac{\partial T}{\partial r}(r,\theta,z)\Big|_{fluide}=k_s\frac{\partial T}{\partial r}(r,\theta,z)\Big|_{solide}$$

For the heated blocks the flux q" is defined versus the volumetric heat generation Q_v and the volume of the block.

As: q" = Qv.V [W], V is the volume of the block.

2.3 Calculation of the Nusselt number

The convective heat transfer rate in the annular space is obtained by the calculation of the Nusselt number, which reflects the ratio of the convective and conductive heat transfers. It is defined as follows:

$$Nu=\frac{hD}{k_f}$$

where h is the heat transfer coefficient at the block, D is the characteristic diameter and k_f is the thermal conductivity of the fluid.

We are interested only in heat transfer at the level of the heated blocks. The Nusselt number can be written depending on the temperature of the heated wall and the fluid in each section as follows:

$$Nu(\theta,z)=\frac{h(\theta,z)D}{k_f}=\frac{D}{k_f}\frac{1}{\left(T_p(r,\theta,z)-T_b(z)\right)}\frac{\partial T}{\partial r}\Big|_{r=Re1} \tag{7}$$

Tp(r, θ, z) is the local temperature of the blocks.

Tb (z) is the bulk temperature in the section (r – θ) is computed as:

$$T_b(z)=\frac{\int_0^{R_1}\int_0^{\pi}T_p(r,\theta,z)rdrd\theta}{\int_0^{R_1}\int_0^{\pi}rdrd\theta} \tag{8}$$

The average Nusselt number is computed on heated walls as

$$\overline{Nu}_{block1,2,3,5}=\frac{\sum_{nodes}Nu_{local(block1,2,3,5)}}{n}=\frac{\sum Nu}{n}\Big|_{block1,2,3,5}$$

With n: is nodes number.

The characteristic parameter of natural convection is set by the Rayleigh number, defined by:

$$Ra = \frac{g\beta Q_v D_h^5}{v\alpha k_f}$$

where g, β, ν, α are respectively the gravitational acceleration, the coefficient of thermal expansion, the kinematic viscosity and the thermal diffusivity, Q_v is the volumetric heat generation and D_h is the hydraulic diameter.

2.4 Resolution procedure

The continuity, momentum and energy equation are solved using commercially software Fluent 6.3 (2006), the simple algorithm proposed by Patankar (1980) is used for coupling between pressure and velocity with a power-law approximation scheme, a numerical solution is supposed to converge when the following test is checked.

$$\left|\frac{\left(\Phi^{k+1} - \Phi^{k}\right)}{\Phi^{k+1}}\right|_{max} \leq 10^{-6}$$

i.e., the residues for different physical quantities become more low 10^{-6}.

Φ_k are u, v, w, T and p, k is the number of iterations.

A non-uniform mesh in axial and radial directions is more refined in regions where temperature variations are relatively important (near the walls). Figure 3 shows mesh structure of the computational domain for $\phi = 0°$ and N = 2.

Figure 3 Mesh structure of the computational domain for $\phi = 0$, N = 2

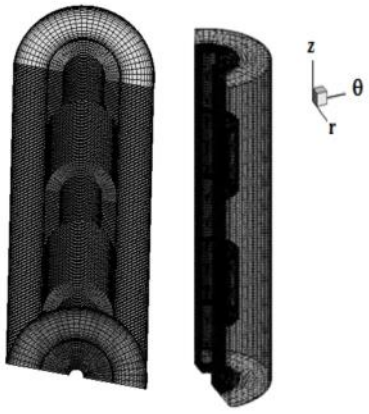

To examine the effect of the mesh on the numerical solution, three meshes have been considered (15 × 20 × 100) nodes, (35 × 30 × 200) nodes and (40 × 30 × 250) nodes. Table 1 gives the values of the average Nusselt number ($\overline{Nu}$) as well as the computing times of each one for the configuration $\phi = 0$ with N = 2 and $Ra = 1.2 \cdot 10^5$. From these results we can see that the values obtained for these different meshes are very close, the mesh size (40 × 30 × 250) give a very precise result but require a higher execution time compared to the others. Our choice was directed towards the grid (35 × 30 × 200) which ensures a good compromise between the computing time and the precision of the results.

Table 1 Variation of $\overline{Nu}$ for various grids for $\phi = 0$, N = 2, $Ra = 1.2.10^5$

Mesh	15 × 20 × 100	35 × 30 × 200	40 × 30 × 250
Time of computing	30 min	1 h	5 h 30 min
$\overline{Nu}$	4.623	5.649	5.788

Figure 4 shows the evolution of the local Nusselt number at the level of the two solids for these three types of mesh. According to these figures we see that the plots of the local Nusselt number for meshes (35 × 30 × 200) and that of (40 × 30 × 250) are identical which confirms our choice of mesh (35 × 30 × 200). The quantitative results are compared with those of Vahl Davis et al. (1969) and Kumar (1991, 1997), for an annular vertical cylinders with the geometrical parameters (A: aspect ratio and $\lambda = r_e/r_i$: the radius ratios). Results of Table 2 show that our results are in agreement with those of literature with a percentage between 8% and 9%.

Table 2 Comparison of $\overline{Nu}$ for annular cylinder (A = 1, λ = 1)

Ra	10^3	10^4
De Vahl Davis (1969)	2.242	4.523
Kumar and Kalam (1991)	2.242	4.523
Kumar (1997)	2.256	4.526
Our results	2.471	4.968

Figure 4 Effect of the mesh on the local Nusselt number for the two blocks (see online version for colours)

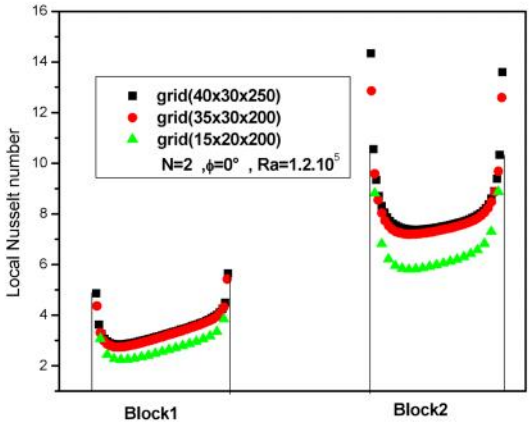

3 Results and discussions

Numerical results of temperature distributions, for various numbers of blocks N (N = 1, 2, 3 and 5) and various inclinations angle of the divergent ($\phi = 0°$, 15°, 23° and 45°)

have been made for the Rayleigh numbers Ra = 1.10^5 and Ra = 2.10^5 corresponding to the volumetric heat generation Q_v = 60,000 W/m^3 and 90,000 W/m^3. Figure 5 illustrates the temperature contours fields in the span-wise direction of the flow for a Rayleigh number Ra = 2.10^5 and N = 3 and for the different inclination angle of the divergent. According to this figure it can be seen that, the natural convection starts when the cold fluid enters towards the annular space between the two cylinders the temperature of the fluid and of the heated blocks increases in the direction of main flow and reach a maximum near the last block in the top. For $\phi = 0°$, i.e., a vertical duct, the fluid layers are concentric circles which temperature decreases in moving away from the blocks and the flow is symmetrical on both sides of the median plane of the duct .

The maximum temperature is near the last block and it is about 373.47 K. For $\phi = 15°$, 23° and 45°, we see a decrease in temperature followed by asymmetry of the flow, the temperature reaches 318.52 K for $\phi = 15°$, 314.78 K for $\phi = 23°$ and 314.26 K for $\phi = 45°$.This is because of the expansion of the fluid due to the sudden enlargement of the divergent outer cylinder of the duct.

Figure 6 shows the velocity contour fields for the configurations and the Rayleigh number considered, from this figure it can be seen that for $\phi = 0°$ the maximum of the velocity is in the middle of the annular space and near the heated blocks mainly in the edges of the second and the last block, it is seen by a plume in this place. The asymmetry of the right top, i.e., on the plume where the flow is more intense, near the blocks where the vectors are diverted to change direction, in the recirculating region where the flow is reversed and its intensity is decreasing.

Figure 5 Temperature contour fields in the span-wise direction of the flow for Ra = 2.10^5, N = 3, (a) $\phi = 0°$ (b) $\phi = 15°$ (c) $\phi = 23°$ (d) $\phi = 45°$ (see online version for colours)

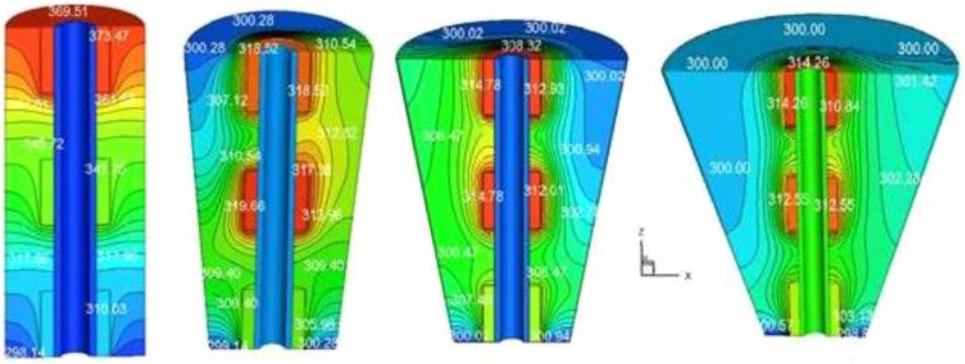

(a) (b) (c) (d)

Figure 6 Velocity contour fields in the span-wise direction of the flow for Ra = 2.105, N = 3, (a) $\phi = 0°$ (b) $\phi = 15°$ (c) $\phi = 23°$ (d) $\phi = 45°$ (see online version for colours)

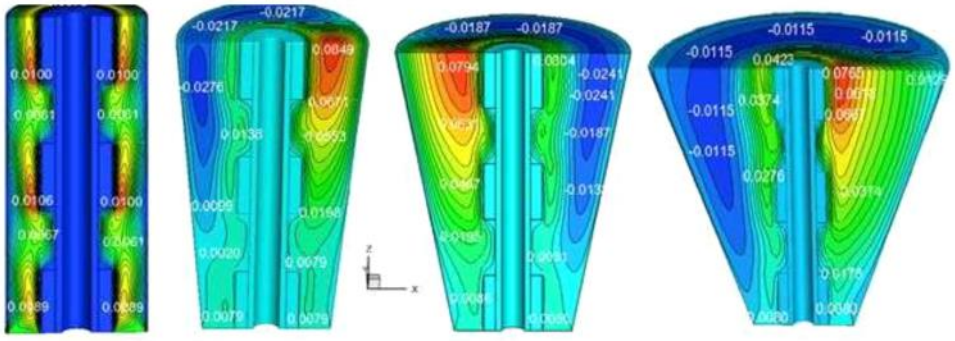

(a) (b) (c) (d)

In Figure 8 for Ra = 2.10^5 and N = 3, the stream lines for different inclination ϕ are depicted. For $\phi = 0°$ the stream lines are a vertical lines in the span-wise direction of the flow and symmetrical from both sides of the inner cylinder. Further for $\phi = 15°$, 23° and 45° the stream lines are not.

The flow is visible by the moving of the plume in the top at the left for $\phi = 23°$ and at the right for $\phi = 15°$and $\phi = 45°$a recirculating cell covering the whole of the duct is formed for $\phi = 15°$, 23° and $\phi = 45°$. The increasing of the inclination angle ϕ leads to a weak buoyancy force due to a weak flow. To see more details on the flow structure, Figure 7 shows the velocity vectors in different area for $\phi = 15°$, in symmetrical and show the reversed flow in the recirculating region for this configurations.

In Figure 9 the velocity and temperature profiles in the annular space in the symmetry plane in the middle of each block are depicted.

For $\phi = 0°$, the highest temperatures are localised in the last block in the top, the velocity profile in this case is parabolic and the flow is fully developed in the span-wise direction of the flow. For $\phi = 15°$, the asymmetry of the flow is visible in both velocity and temperature profiles. The plume produced by the buoyancy forces that carry the fluid particles in the top under the effect of heat where the highest velocities are located. This plume is translated by the velocity and temperature profiles disturbed in the direction of flow for $\phi = 15°$, 23° and 45°due to the change in the outlet section thus causing a decrease in the temperature.

Figure 7 Velocity vectors in different areas for $\phi = 23°$, N = 3, Ra = 2.10^5

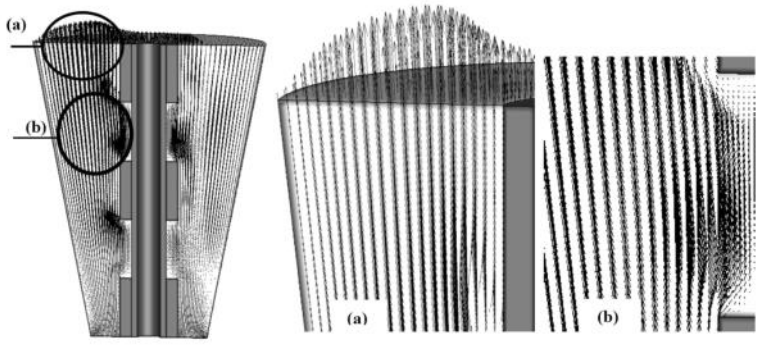

Figure 8 Effect of the inclination angle on streamlines for Ra = 2.10^5, N = 3, (a) $\phi = 0°$ (b) $\phi = 15°$ (c) $\phi = 23°$ (d) $\phi = 45°$

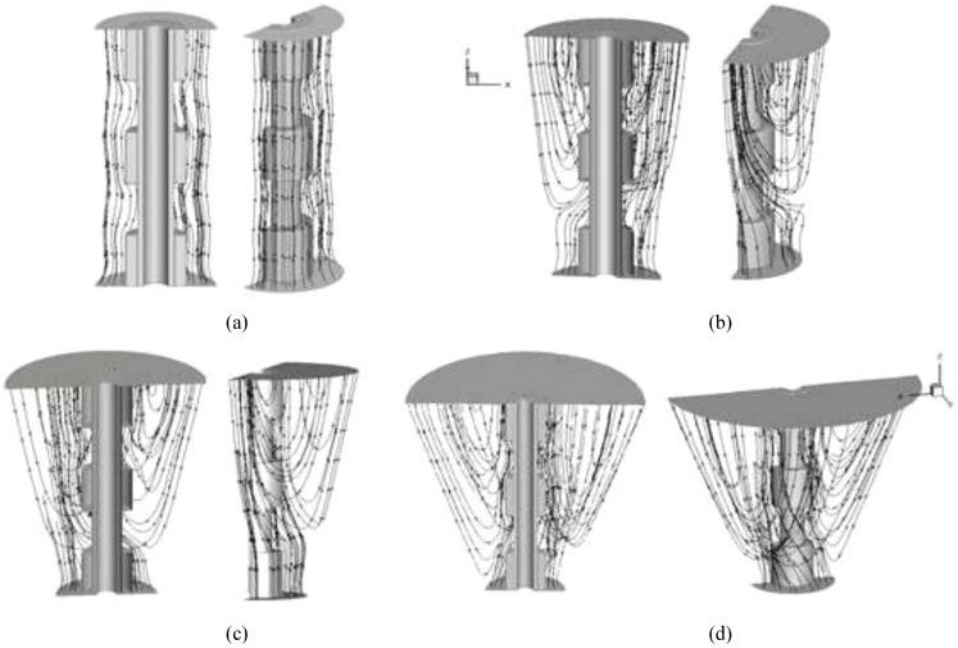

Figure 9 Velocity and temperature profiles in the symmetry plane (x, z) in the middle of each block, N = 3, Ra = 2.10^5, (a) $\phi = 0°$ (b) $\phi = 15°$ (c) $\phi = 23°$ (d) $\phi = 45°$ (see online version for colours)

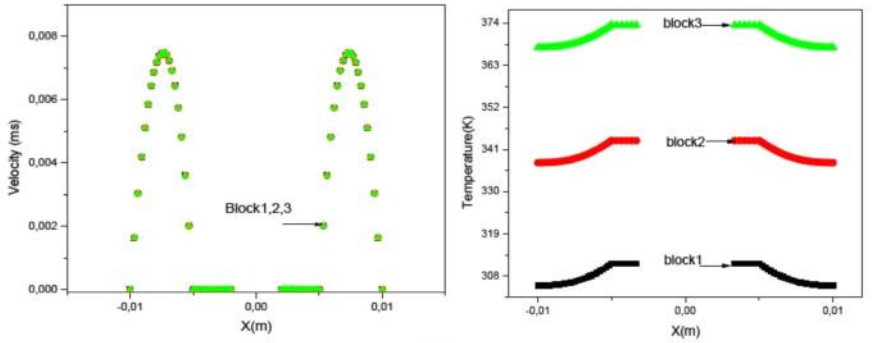

(a)

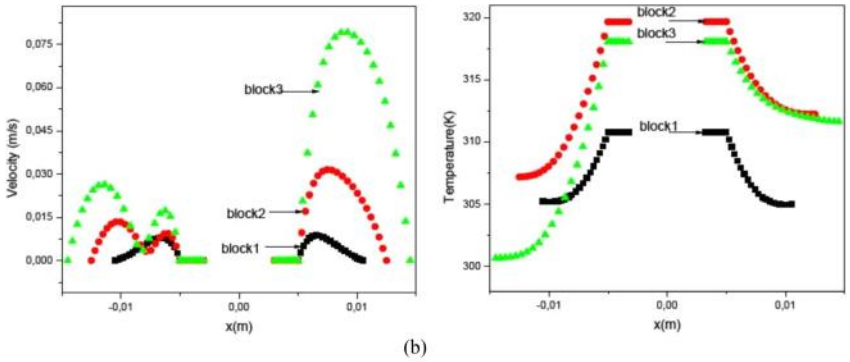

(b)

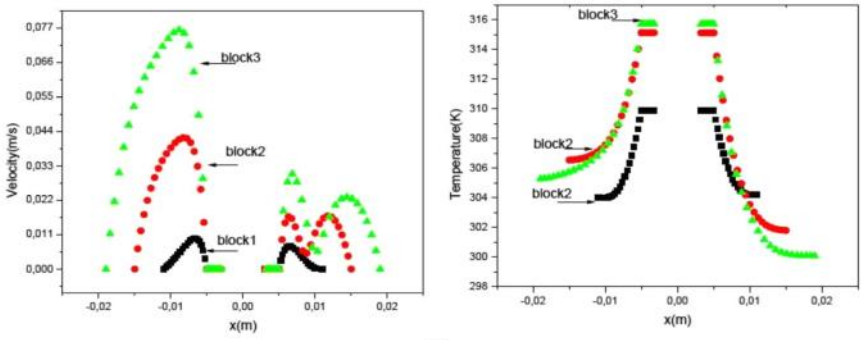

(c)

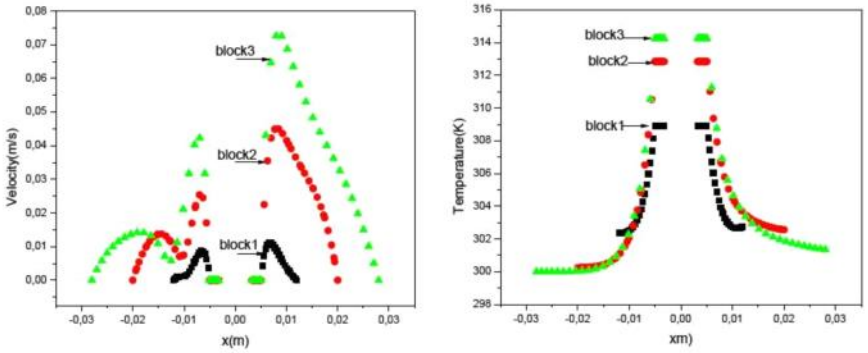

(d)

Figure 10 Velocity and temperature profiles in a vertical line near the surface of the blocks for N = 3, Ra = 2.10^5 (see online version for colours)

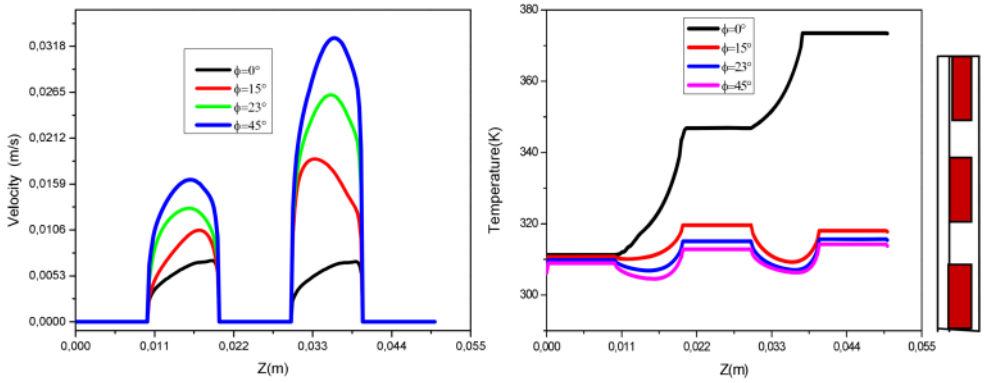

Further the highest temperatures are localised in the top at the level of the second and the third block.

Figure 10 exemplifies the variation of the velocity and temperature profiles in a vertical line near the surface of the blocks in the span-wise direction of the flow. It is shown from this figure that for both temperature and velocity the trends are similar. For $\phi = 0°$, the temperature is high and the maximum is in the top at the level of the last block. Further for $\phi = 15°$, 23° and 45°, the decrease in temperature leads to an increase of the velocities. Figure 11 presents the variation of the local Nusselt number at the heated blocks for these configurations and for N = 3. It is shown that the Nu profiles present an increasing in the level of the last block and for inclination angles $\phi \neq 0$; this is due to the fact that with increasing the inclination angle ϕ, the convection increases progressively.

Figure 11 Variation of the local Nusselt number on the heated blocks (see online version for colours)

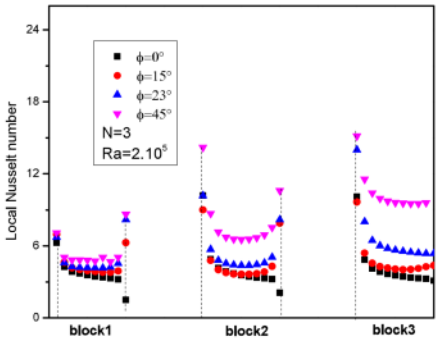

To show the influence of the numbers of blocks N and ϕ on the structure of the flow we have considered necessary to plot the velocity and temperature profiles in a vertical line near the blocks also and in the symmetry plane for N = 1, 2, 3 and N = 5 . Figure 12 illustrates the variation of the velocity and the temperature profiles in the span-wise direction of the flow in a vertical line near the surface of the blocks for a number N = 1, 2, 3 and 5 blocks and for Ra = 1.10^5.

It can be seen from these plots that the temperature remains high for $\phi = 0°$ and for the different number of N. Further the maximum temperature is in the top near the last block where as for N = 2, 3 and 5 slight difference between plots appears. This temperature decreases for $\phi = 15°$, 23° and 45° for the different number of blocks, also seen in Figure 13 which shows the velocity and temperature profiles in the annular space in the symmetry plane and in the middle of each block . On the other part it is indicated from these figures that the enhanced fluid velocity increases with the number of the heated blocks and the inclination angle ϕ. The highest velocities are in the middle of the annular space and zero at the level of the walls of the heated blocks.

Figure 14 illustrates the variation of the local Nusselt number along the heated wall of the block. The plots are presented for different number N of blocks to understand the effect of the blocks and the inclination angle ϕ on the characteristics of the flow .It can be seen from this figure that the local Nusselt number is an increasing function of the inclination ϕ and it is seen that the trends are similar. On the other part the maximum value of Nu is located on the edges of the blocks, it is about 17 for N = 1 and $\phi = 45°$at the level of the first edge and it reaches the value of 14 at the second block for N = 2 and $\phi = 45°$, the highest values of the local Nusselt number correspond to N = 1 and $\phi = 45°$ then the local Nusselt number is a decreasing function of N.

Figure 15 shows the variation of the average Nusselt number versus the numbers N of blocks and for the inclination angles ϕ studied. From this figure it is shown that the average Nusselt number is a decreasing function of the number of blocks N and an increasing function of the inclination angle ϕ.

Figure12 Variations of the velocity and temperature pro files in a vertical line near the surface of the blocks for, Ra = 1.10^5, (a) N = 1 (b) N = 2 (c) N = 3 (d) N = 5 (see online version for colours)

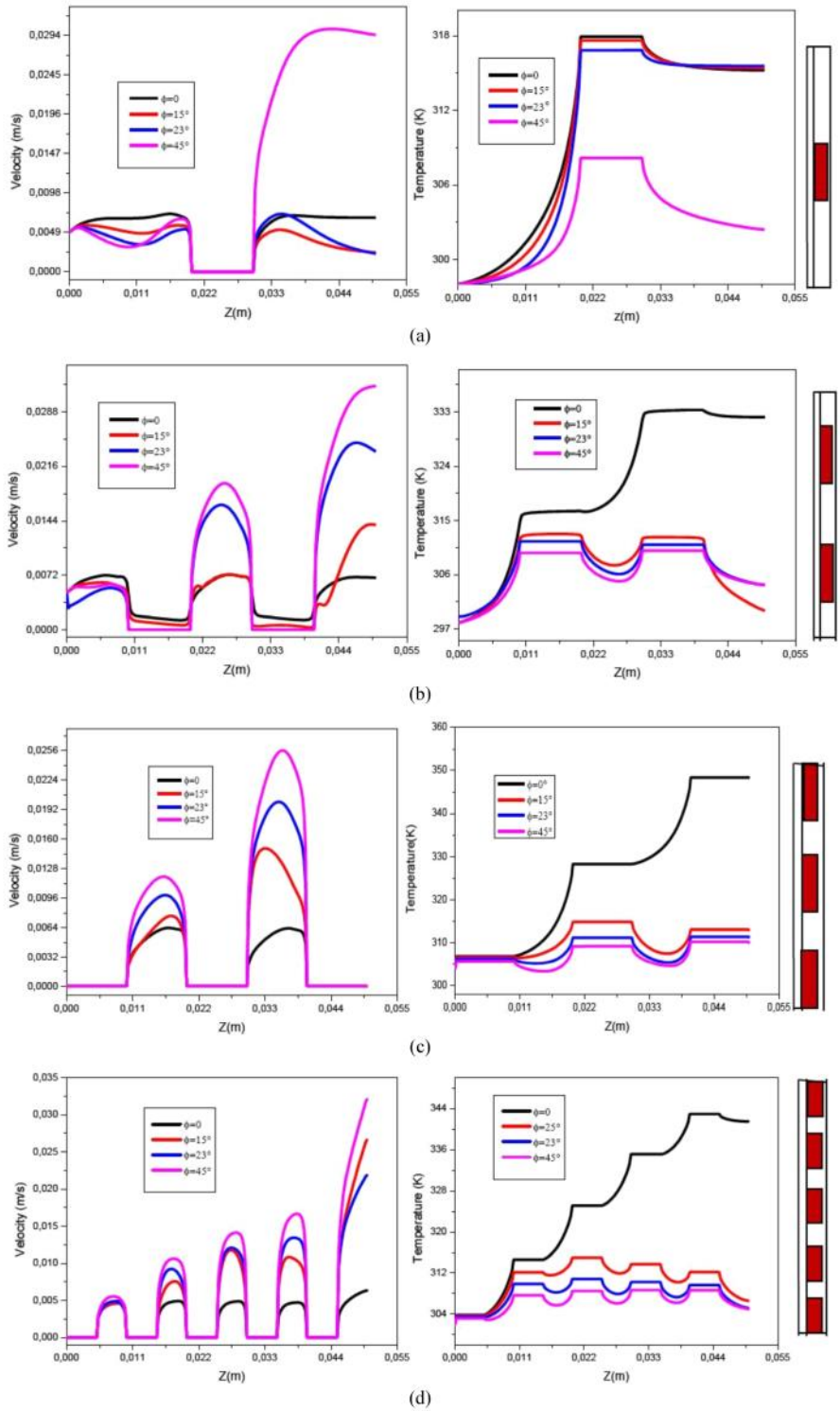

Figure 13 Velocity and temperature profiles in the symmetry plane (x, z) in the middle of each block, Ra = 1.10^5, (a) N = 1 (b) N = 2 (c) N = 3 (d) N = 5 (see online version for colours)

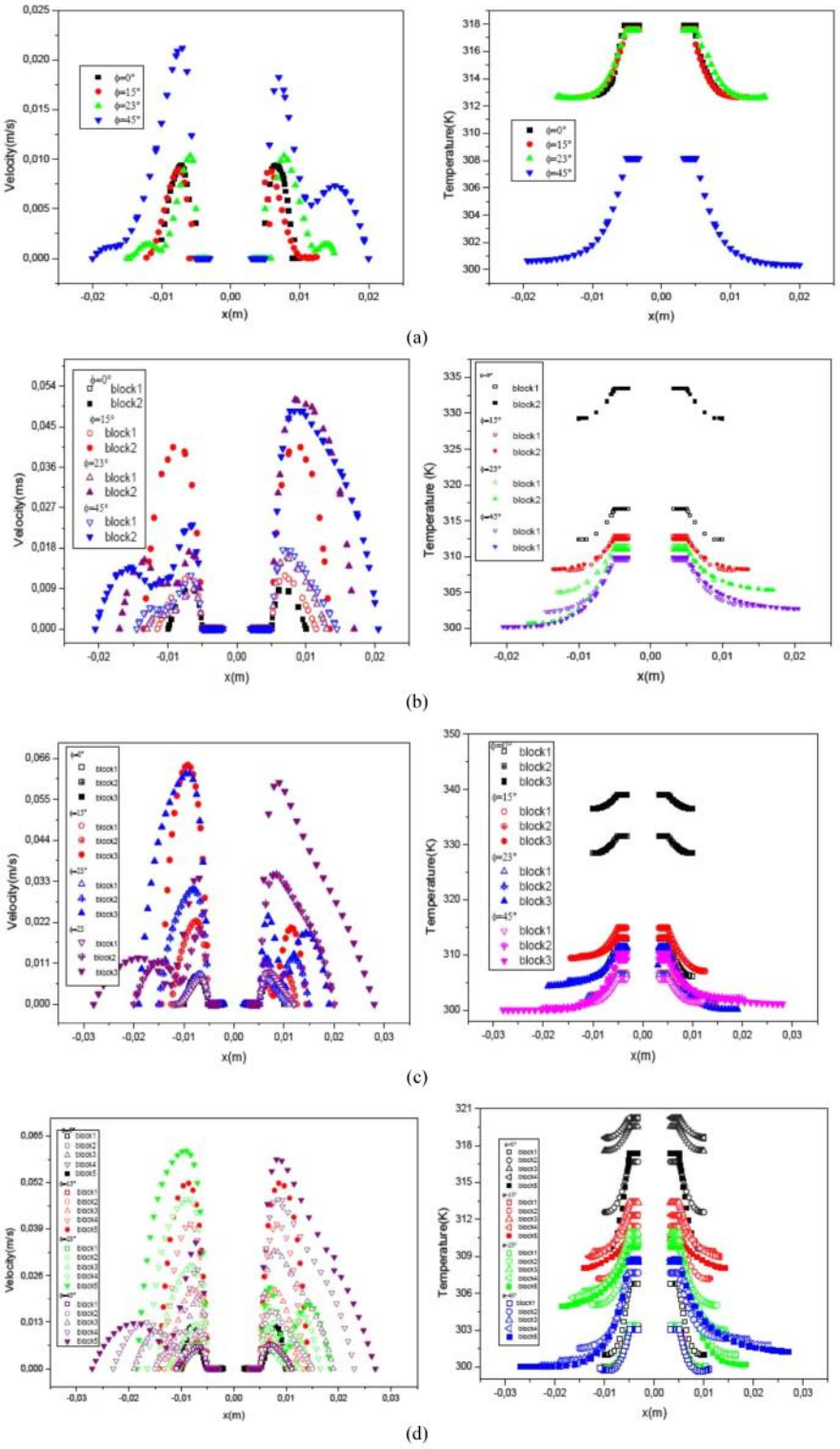

Figure 14 Local heat transfer rate for Ra = 1.10^5 (see on line version for colours)

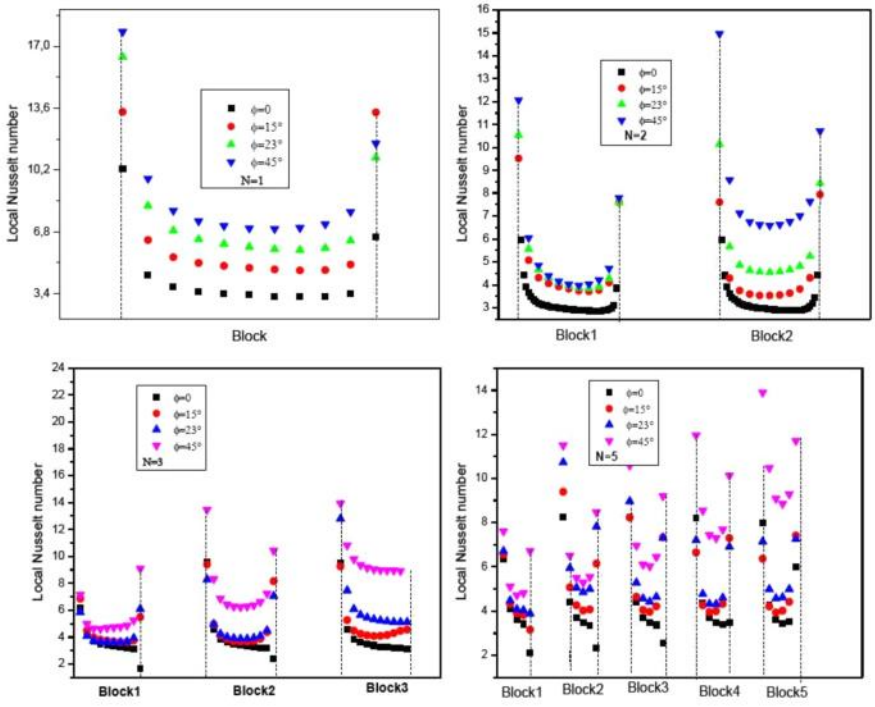

Figure 15 Average Nusselt number versus the number of blocks (see online version for colours)

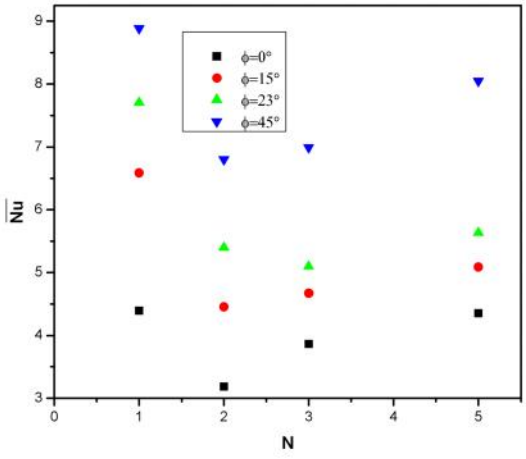

4 Conclusions

The numerical study of natural convection heat transfer and fluid flow in a 3D cylindrical and divergent annular duct has been presented. Heated blocks are attached in the inner cylinder and are subjected of a volumetric heat generation. The effect of the numbers of heated blocks (N = 1, 2, 3 and 5) and the inclination angle of the divergent (ϕ = 0, 15°, 23° and 45°) have been studied.

The result of numerical simulation for Ra = 1.10^5 and Ra = 2.10^5 leads to the following conclusions.

- the temperature decreases with the increasing of the inclination angle ϕ
- a loss of symmetry particularly when ϕ is high is observed in the velocity and the temperature contours fields
- the temperature of the flow increases with the number of the heated blocks, except for N = 5, where the temperature decreases
- the maximum temperature is at the level of the last block in the top for the all inclination angles
- the local Nusselt number is an increasing function of the inclination angle while the average Nusselt number is a decreasing function of the heated blocks N.

References

Bazylak, A., Djilali, N. and Sinton, D. (2007) 'Natural convection with distributed heat sources Modulation', *Int. J. of Heat and Mass Transfer*, Vol. 50, Nos. 9–10, pp.1649–1655.

Bejan, A. (1995) *Convection Heat Transfer*, 2nd ed., July 17, John Wiley & sons Inc., New York, USA.

Biber, C.R. and Camparella, V. (2001) 'Convoluted fin heat sinks with base topography for thermal enhancement', U.S. Patent No. 6,260,610, 17 July.

Chen, H.T. and Hsu, W.L. (2007) 'Estimation of heat transfer coefficient on the fin of annular-finned tube heat exchangers in natural convection for various fin spacing', *Int. J. of Heat and Mass Transfer*, Vol. 50, Nos. 9–10, pp.1750–1761.

Culham, J.R., Teertstra, P. and Yovanovich, M.M. (2000) 'Natural convection modeling of heat sinks using web-based tools',*Electronics Cooling*, 1 September, Vol. 6, No. 3, pp.44–51.

Dehghan, A.A. and Behnia, M. (1996) 'Numerical investigation of natural convection in a vertical slot with two heat source elements ', *Int. J. Heat and Fluid Flow*, Vol. 17, No. 5, pp.474–482.

De Vahl Davis, G. and Thomas, R.W. (1969) 'Natural convection between concentric vertical cylinders', *High Speed Computing in Fluid Dynamics Physics of Fluids*, Supplement II, pp.198–207.

Edward, J.A. and Chaddock, J. (1963) 'Experimental investigation of radiation and free convection heat transfer from a cylindrical disk extended surface', *AchraE*, Vol. 69, pp.313–319.

Fluent 6.3 (2006) *User's Guide*, Fluent Inc.

Kasayapanand, N. (2009) 'A computational fluid dynamics modeling of natural convection in finned enclosure under electric fields', *Applied Thermal Engineering*, Vol. 29, No. 1, pp.131–141.

Kobus, C.J. and Toshio, A. (2005) 'Development of a theoretical model for predicting the thermal performance characteristics of a vertical pin-fin array heat sink under combined forced and natural convection with impinging flow', *Int. J. Heat and Mass Transfer*, Vol. 48, No. 6, pp.1053–1063.

Kumar, R. (1997) 'Three dimensional natural convective flow in vertical annulus with longitudinal fins', *Int. J. of Heat and Mass Transfer*, Vol. 40, No. 14, pp.3323–3334.

Kumar, R. and Kalam, M.A. (1991) 'Laminar thermal convection between coaxial vertical isothermal cylinders', *Int. J. Heat and Transfer*, Vol. 34, No. 2, pp.513–524.

Mahmoudi, A.H., Shahi, M., Honarbakhsh, A.R. and Ghasemian, A. (2010) 'Numerical study of natural convection cooling of horizontal heat source mounted in a square cavity filled with Nano fluid', *Int. Com. in Heat and Mass Transfer,* Vol. 37, No. 8, pp.1135–1141.

Patankar, S.V. (1980) *Numerical heat Transfer and Fluid Flow*, McGraw-Hill, New York.

Rasim, K. (1996) 'Experimental relationships for heat flux, Nusselt number and temperature difference in a finned heater', *Energy. Convers. MgM.*, Vol. 37, No. 5, pp.591–597.

Wang, C-S., Yovanovich, M.M. and Culham, J.R. (1999) 'General model for natural convection: application to annular-fin heat sinks', *ASME Journal of Electronic Packaging*, Vol. 121, No. 1, pp.44–49.